Inorganic Chemistry

Article

pubs.acs.org/IC

Cyclometalated Platinum(II) Terpyridylacetylide with a Bis(arylamine) Donor as a Proton-Triggered Luminescence Chemosensor for Zn^{2+}

Dongfang Qiu,* Mengmeng Li, Qian Zhao, Hongwei Wang, and Chunxia Yang

College of Chemistry and Pharmacy Engineering, Nanyang Normal University, Nanyang, 473061, P. R. China

Supporting Information

ABSTRACT: A cyclometalated Pt(II) acetylide derivative bearing a bis(arylamine) donor (D) and a terpyridine (TPY) receptor (A) was successfully synthesized and characterized. This three-component D−π−A system displays an intense low-energy absorption band at λ_{max} = 470 nm, resulting from overlapping the dπ(Pt) → π*(C^N^N) metal-to-ligand charge transfer and π(C≡C−Ar) → π*(C^N^N) ligand-to-ligand charge transfer transitions with the π(bis(arylamine)) → π*(C^N^N) intraligand charge transfer transition. Upon protonation of the bis(arylamine) donor, a strong emission from the phosphorescence Pt(II) complex unit is recovered at λ_{max} = 580 nm. With introduction of the TPY receptor, this complex possesses quite high affinity for Zn^{2+} ($K_a = 6.86 \times 10^9$ $mol^{-2}\cdot dm^6$) to form the heterotrinuclear Pt−Zn−Pt complex in CH_2Cl_2 solution. Though this coordination effect is seriously inhibited by protons in acidic medium, the 2.4-fold luminescence intensity enhancement is obtained yet, strongly suggesting the presence of the intramolecular energy transfer process from the Zn(II)-TPY complex core to the phosphorescence Pt(II) complex units at two ends. The H^+-triggered and Zn^{2+}-enhanced luminescence can be reversibly switched on and off upon successive additions of H^+ and OH^-. Furthermore, this complex displays an unexpected Zn^{2+}-selective luminescence enhancement effect in acidic solution.

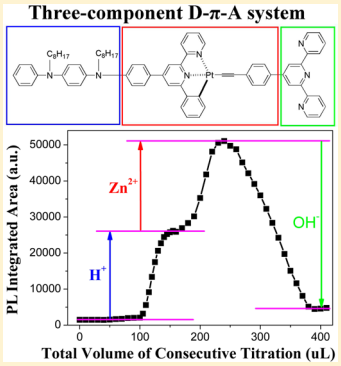

INTRODUCTION

Zinc, known as the element of life, is involved in important physiological functions in living organisms. A number of diseases are regarded as being associated with zinc deficiency or overcapacity in human body.[1] Therefore, the sensitive detection of zinc ion in living organisms and their closely contacted environment and food samples is of utmost importance for human health.

Because luminescent chemosensors generally possess high sensitivities, low detection limits, and attractive potentials in the in vivo bioimaging application,[2] a number of "chromophore−spacer−receptor" systems that can selectively recognize Zn^{2+} at their receptor sites and can produce measurable luminescence changes have been established.[3] However, the use of organic fluorophores in these systems may be limited by their small Stokes shifts and short fluorescence lifetimes, as well as autofluorescence arising in biological samples. In this context, transition metal complexes with multiple electronic transitions in visible region, high phosphorescence quantum efficiencies, and long lifetimes have been widely employed as fluorophores in chemosensors for Zn^{2+}.[4]

Recently, square-planar polypyridine platinum(II) complexes have attracted much attention in luminescence ion-binding studies, because of their intriguing spectroscopic and luminescent properties as well as their favorable structure and electronic conditions for fast electron/hole or exciton migration.[5] A series of platinum(II) terpyridyl complexes imparted with metal-binding units have been reported that display colorimetric and/or luminescent responses toward various protons and cations.[6] The terpyridine (TPY) platinum(II) σ-alkynyl complex with a TPY receptor[7] and cyclometalated platinum(II) σ-alkynyl complex with a bis(2-picolyl)aniline (DPA) receptor[8] have also been used in such investigation, but these systems suffer the problem of insufficient selectivity for Zn^{2+} over other coexisting transition metal ions, especially Cd^{2+}.

Herein, we report a novel three-component donor−π−acceptor (D−π−A) system (Chart 1, complex **2**), in which the cyclometalated Pt(II) acetylide core serves as a planar π-conjugated chromophore, the bis(arylamine) moiety serves as a rich electron-donating component, and the pendant TPY unit serves as a strong electron-withdrawing acceptor and a general receptor for transition metal ions. Its synthesis, photophysical properties, and multichannel luminescence behaviors are mainly discussed with complex **1** as a reference compound.

EXPERIMENTAL SECTION

Materials and General Procedures. All starting materials, 2-acetylpyridine, 4-bromobenzaldehyde, ammonium formate, *p*-aminodiphenylamine, benzophenone, palladium acetate ($Pd(OAc)_2$), sodium *tert*-butoxide (NaO^tBu), bis[(2-diphenylphosphino)phenyl]ether (DPEphos), di-*tert*-butyl bicarbonate ($(BOC)_2O$), 4-(dimethylamino)-pyridine (4-DMAP), palladium on carbon (Pd/C, 10%), NaH (>52%, in mineral oil), 1-bromooctane, triphenylphosphine (PPh_3), (trimethylsilyl)acetylene, anhydrous K_2CO_3, CuI, K_2PtCl_4, and phenylacetylene ($C_6H_5C{\equiv}CH$) were purchased from commercial

Received: April 4, 2015
Published: July 28, 2015

DOI: 10.1021/acs.inorgchem.5b00756
Inorg. Chem. 2015, 54, 7774−7782

Chart 1. Molecular Structure of Complexes 1 and 2

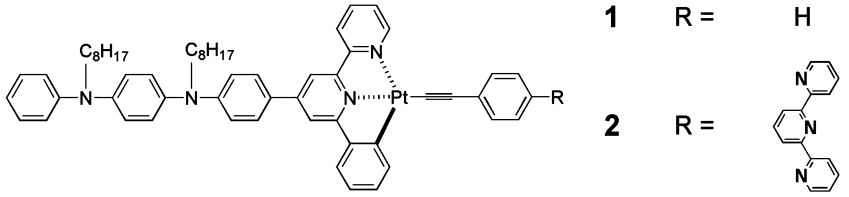

sources and used as received without further purification. Reactions under an argon atmosphere were performed in oven-dried glassware using standard Schlenk techniques. The solvents used for synthesis were of analytical grade. Tetrahydrofuran (THF) was distilled under argon from sodium benzophenone ketyl. Toluene was distilled under argon from molten sodium. Diisopropylamine was treated with 5 Å molecular sieves and distilled under reduced pressure. All metal salts, such as $Zn(ClO_4)_2$, $Cd(ClO_4)_2$, $Fe(ClO_4)_2$, $NaClO_4$, $KClO_4$, $Ca(CH_3COO)_2$, $Mg(CH_3COO)_2$, $Mn(CH_3COO)_2$, $Co(CH_3COO)_2$, $Ni(CH_3COO)_2$, $Cu(CH_3COO)_2$, and $Pb(CH_3COO)_2$, were analytical reagent grades and used as supplied to prepare the titrant CH_3OH solutions containing 3.5×10^{-3} mol·dm^{-3} metal ions, respectively. The supporting electrolyte for the electrochemical studies, tetrabutylammonium perchlorate ($^n Bu_4NClO_4$), was prepared by the metathesis of tetrabutylammonium bromide and perchloric acid. The electrolyte was recrystallized from hot pentanol/ethyl acetate solution twice, giving colorless crystals, and dried in a vacuum oven. ***Caution!*** *Perchlorate salts are potentially explosive and should be handled with care and in small amounts.*

Syntheses of 4-(*p*-bromophenyl)-6-phenyl-2,2′-bipyridine, 4-phenyl-6-phenyl-2,2′-bipyridine (ph-C^N^N), [(ph-C^N^N)Pt(C≡C−C_6H_5)],[9a] 4′-phenyl-2,2′:6′,2″-terpyridine (ph-TPY), [Zn(ph-TPY)$_2$]-$(PF_6)_2$,[9b] N′-(*tert*-butoxycarbonyl)-*N*′-(phenyl)-*p*-phenylenediamine, and *N*,*N*′-dibutyl-*N*,*N*′-diphenyl-*p*-phenylene-diamine[9c] have been described previously.

Synthesis of 4-{*p*-[*p*-(*N*,*N*′-Dioctyl-*N*′-phenyl)-phenyldiamino]}-phenyl-6-phenyl-2,2′-bipyridine (HL). 4-(*p*-Bromophenyl)-6-phenyl-2,2′-bipyridine (3.87 g, 10.00 mmol), palladium acetate (0.025 g, 0.11 mmol), and DPEphos (0.087 g, 0.16 mmol) were charged into a flask and purged with argon. *N*′-(*tert*-butoxycarbonyl)-*N*′-(phenyl)-*p*-phenylenediamine (3.40 g, 12.00 mmol) was added, followed by toluene (40 mL). NaO^{t}Bu (1.62 g, 16.90 mmol) was added in one portion. The reaction mixture was heated to 80 °C with stirring for 9 h. The solvent was removed by rotary evaporation. The residue was dissolved in CH_2Cl_2, washed with distilled water, and dried over anhydrous sodium sulfate and concentrated. The obtained solid was dissolved in THF (50 mL), and $(BOC)_2O$ (1 M in THF; 16 mL, 16.00 mmol) and 4-DMAP (0.18 g, 1.50 mmol) were added. The reaction mixture was refluxed for 24 h. The solvent was removed, and the BOC-protected ligand H**L** was separated by column chromatography (Al_2O_3, petroleum ether (PE)/CH_2Cl_2 = 5:1 (v/v) containing 5% (v) triethylamine) as white powder in yield of 88%. The obtained intermediate was placed in a flask under argon. The system was heated to 185 °C for 12 h. After it cooled to room temperature, THF (100 mL) was added to dissolve the solid. NaH (4.82 g, >52%, in mineral oil) was added and purged with argon. The reaction mixture was stirred for 1 h at room temperature, and then 1-bromooctane (40.00 mmol) was added dropwise via syringe. The solution was refluxed until the conversion was complete (as monitored by thin layer chromatography). The solution was cooled to room temperature, poured into ice−water mixture slowly, and extracted with CH_2Cl_2 until the water phase was colorless. The combined organic solutions were washed with distilled water, dried over anhydrous sodium sulfate, and concentrated. The crude product was purified by column chromatography (silica gel, PE/CH_2Cl_2 = 7:1 (v/v) to CH_2Cl_2/PE = 4:1 (v/v)). Ligand H**L** was obtained as pale green crystal in yield of 78%. ^{1}H NMR (300 MHz, CD_3COCD_3): δ 8.72−8.69 (m, 3H), 8.35 (d, J = 8.7 Hz, 2H), 8.17 (s, 1H), 7.97 (t, J = 7.5 Hz, 1H), 7.81(d, J = 8.7 Hz, 2H), 7.67 (t, J = 7.5 Hz, 2H), 7.49−7.42 (m, 2H), 7.28 (d, J = 7.8 Hz, 2H), 7.16 (d, J = 8.4 Hz, 2H), 7.06 (broad, 4H), 6.96−6.91 (m, 3H, *Ar*), 3.76 (broad, 4H, α ($-CH_2$)), 1.71 (broad, 4H, β ($-CH_2$)), 1.28 (broad, 20H, γ ($-CH_2$)), 0.97 (broad, 6H, $-CH_3$).

Synthesis of Complex [(L)PtCl]. A mixture of H**L** (0.36 g, 0.50 mmol), K_2PtCl_4 (0.21 g, 0.50 mmol), and glacial acetic acid (50 mL) was refluxed for 12 h under a nitrogen atmosphere in the absence of light. The reaction mixture was then cooled to room temperature and filtered. The obtained solid was recrystallized from CH_3OH/CH_2Cl_2 solution to form desired product. Complex [(**L**)PtCl] was obtained as deep red crystal in yield of 85%. ^{1}H NMR (300 MHz, DMSO-d_6): δ 8.90 (d, J = 4.5 Hz, 1H), 8.69 (d, J = 8.4 Hz, 1H), 8.40 (s, 1H), 8.35 (t, J = 7.8 Hz, 1H), 8.12 (s, 1H), 7.96 (d, J = 9.0 Hz, 2H), 7.89 (t, J = 6.6 Hz, 1H), 7.76 (d, J = 7.5 Hz, 1H), 7.48 (d, J = 7.5 Hz, 1H), 7.29 (t, J = 7.8 Hz, 2H), 7.15−7.00 (m, 8H), 6.94 (t, J = 7.2 Hz, 1H), 6.81 (d, J = 8.7 Hz, 2H, *Ar*), 3.71 (m, 4H, α ($-CH_2$)), 1.60 (broad, 4H, β ($-CH_2$)), 1.24 (broad, 20H, γ ($-CH_2$)), 0.85 (m, 6H, $-CH_3$). Matrix-assisted laser desorption/ionizatin time-of-flight mass spectrometry (MALDI-TOF MS): m/z = 944.1 ([M]$^-$, $C_{50}H_{57}ClN_4Pt$ requires 943.39). Anal. Calcd (%): C, 63.58; H, 6.08; N, 5.93. Found: C, 63.52; H, 5.84; N, 5.62.

Synthesis of [(L)Pt(C≡CC_6H_5)] (1). A mixture of [(**L**)PtCl] (0.28 g, 0.30 mmol), $C_6H_5C{\equiv}CH$ (1 mL), Et_3N (5 mL), and CuI (0.0050 g, 0.026 mmol) in degassed CH_2Cl_2 (50 mL) was stirred for 12 h under an argon atmosphere at room temperature in the absence of light. The reaction mixture was then evaporated to dryness under reduced pressure. The crude product was purified by flash chromatography (neutral Al_2O_3, CH_2Cl_2 as eluent) and recrystallized from CH_2Cl_2/CH_3OH solution to form desired product as red crystal in yield of 84%. ^{1}H NMR (400 MHz, $CDCl_3$): δ 9.01 (d, J = 5.2 Hz, 1H), 7.94−7.87 (m, 3H), 7.62 (s, 1H), 7.54 (t, J = 8.0 Hz, 4H), 7.48 (s, 1H), 7.33 (t, J = 8.0 Hz, 3H), 7.28 (t, J = 7.6 Hz, 3H), 7.16 (t, J = 7.4 Hz, 1H), 7.13−7.07 (m, 5H), 7.03−6.98 (m, 4H), 6.75 (d, J = 8.8 Hz, 2H, *Ar*), 3.73 (t, J = 7.8 Hz, 2H, $\alpha(-CH_2)$), 3.68 (t, J = 7.6 Hz, 2H, $\alpha(-CH_2)$), 1.74−1.69 (m, 4H, $\beta(-CH_2)$), 1.36−1.31 (m, 20H, $\gamma(-CH_2)$), 0.93−0.88 (m, 6H, $-CH_3$). ^{13}C NMR (100 MHz, $CDCl_3$): δ 164.7, 158.2, 154.1, 151.3, 151.0, 150.5, 147.9, 147.2, 145.8, 142.2, 139.1, 138.5, 138.3, 131.8, 130.9, 129.4, 129.2, 127.9, 127.8, 127.7, 126.9, 125.2, 124.8, 123.9, 123.4, 122.7, 121.7, 121.0, 114.8, 114.7, 114.4, 106.4, 106.0, 52.5, 31.8, 29.5, 29.4, 29.3, 27.5, 27.4, 27.1, 27.0, 22.6, 14.1. MALDI-TOF MS: m/z = 1010.5 ([M]+1, $C_{58}H_{62}N_4Pt$ requires 1009.5).

Synthesis of 4′-{4-[2-(Trimethylsilyl)-1-ethynyl]phenyl}-2,2′:6′,2″-terpyridine. A 250 mL round-bottomed Schlenk flask was charged with 4′-(4-bromophenyl)-2,2′:6′,2″-terpyridine (1.94 g, 5.00 mmol), $Pd(OAc)_2$ (0.011 g, 0.049 mmol), CuI (0.011 g, 0.058 mmol), triphenylphosphine (0.034 g, 0.13 mmol), (trimethylsilyl)-acetylene (1 mL, 7.65 mmol), and finally argon-degassed diisopropylamine (120 mL). The mixture was heated at 75 °C under stirring for 24 h. After complete consumption of the starting material, the solvent was evaporated to give a crude product, which was purified by flash chromatography on silica gel, eluting with CH_2Cl_2/CH_3OH. Recrystallization from CH_2Cl_2/CH_3OH obtained the desired compound as white crystal in yield of 86%. ^{1}H NMR (300 MHz, $CDCl_3$): δ 8.74−8.72 (m, 4H), 8.66 (d, J = 7.8 Hz, 2H), 7.90−7.84 (m, 4H), 7.61 (d, J = 8.4 Hz, 2H), 7.35 (dd, J = 4.8 Hz, 2H, *Ar*), 0.29 (s, 9H).

Synthesis of 4′-(4-Ethynylphenyl)-2,2′:6′,2″-terpyridine (H-C≡C-PTPY). To a stirred solution of 4′-{4-[2-(trimethylsilyl)-1-ethynyl]phenyl}-2,2′:6′,2″-terpyridine (0.41 g, 1.01 mmol) in CH_3OH/THF (1/1, v/v) was added anhydrous K_2CO_3 (0.18 g, 1.30 mmol) as a solid. After complete consumption of the starting

DOI: 10.1021/acs.inorgchem.5b00756
Inorg. Chem. 2015, 54, 7774−7782

Scheme 1. Synthetic Routes of HL, 1, and 2

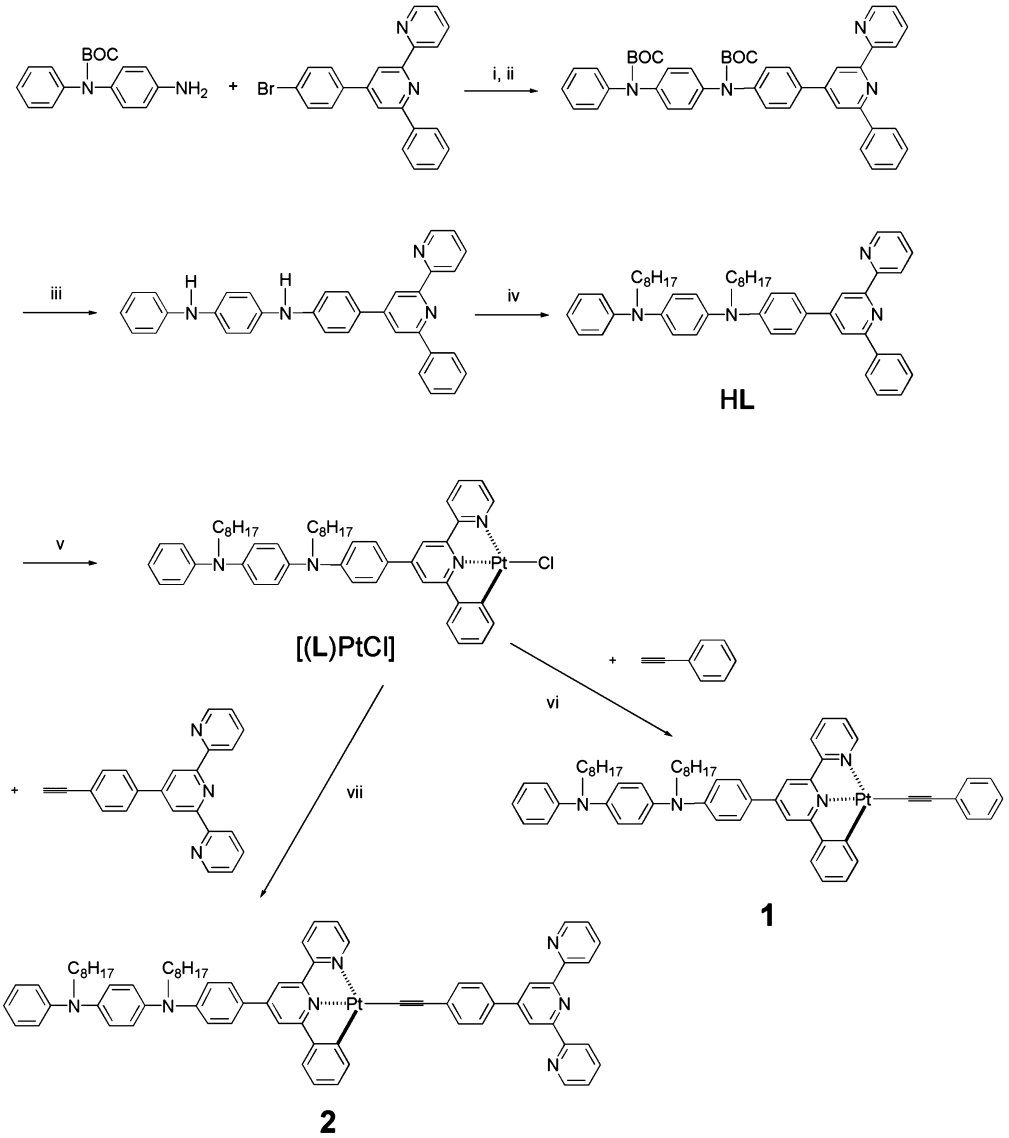

material, the solution was concentrated by rotary evaporation to give a crude product, which was purified by flash chromatography on silica gel eluting with CH_2Cl_2/CH_3OH. The desired compound was obtained as white powder in yield of 91%. ^1H NMR (300 MHz, $CDCl_3$): δ 8.76 (m, 4H), 8.69 (d, J = 7.9 Hz, 2H), 7.93−7.87 (m, 4H), 7.66 (d, J = 8.4 Hz, 2H), 7.38 (dd, J = 4.8 Hz, 2H), 3.22 (s, 1H).

Synthesis of [(L)Pt(C≡C-PTPY)] (2). To a stirred solution of [(**L**)PtCl] (0.16 g, 0.17 mmol) and 4′-(4-ethynylphenyl)-2,2′:6′,2″-terpyridine (0.060 g, 0.18 mmol) in degassed CH_2Cl_2 (20 mL), CuI (0.0054 g, 0.028 mmol) and Et_3N (4 mL) were successively added. The mixture was stirred for 24 h under an argon atmosphere at room temperature in the absence of light and then evaporated to dryness under reduced pressure. The crude product was purified by flash chromatography (neutral Al_2O_3, CH_2Cl_2 as eluent) and recrystallized from CH_2Cl_2/CH_3OH solution to form desired product as orange powder in yield of 89%. ^1H NMR (400 MHz, $CDCl_3$): δ 9.16 (d, J = 5.2 Hz, 1H), 8.80 (s, 2H), 8.76 (s, 1H), 8.75 (s, 1H), 8.69 (d, J = 8.0 Hz, 2H), 8.02−7.87 (m, 7H), 7.69 (s, 1H), 7.68 (d, J = 8.0 Hz, 2H), 7.58 (t, J = 8.2 Hz, 3H), 7.48 (t, J = 6.2 Hz, 1H), 7.39−7.34 (m, 3H), 7.31 (t, J = 7.8 Hz, 2H), 7.19 (t, J = 7.2 Hz, 1H), 7.10−7.06 (m, 5H), 7.02−6.97 (m, 3H), 6.80 (d, J = 8.8 Hz, 2H, *Ar*), 3.72−3.66 (m, 4H, $\alpha(-CH_2)$), 1.74−1.69 (broad, 4H, $\beta(-CH_2)$), 1.33−1.27 (m, 20H, $\gamma(-CH_2)$), 0.90−0.87 (m, 6H, $-CH_3$). ^{13}C NMR (100 MHz, $CDCl_3$): δ 164.4, 158.1, 156.4, 155.8, 154.1, 151.2, 150.9, 150.5, 150.1, 149.1, 147.9, 147.2, 145.7, 142.2, 139.1, 138.4, 138.3, 136.7, 134.3, 132.3, 130.8, 130.3, 129.3, 127.9, 127.8, 126.9, 126.7, 125.1, 123.9, 123.7, 123.4, 122.8, 121.6, 121.5, 121.3, 121.2, 118.4, 114.9, 114.6, 114.3, 110.2, 105.9, 52.5, 31.8, 29.5, 29.4, 29.3, 27.5, 27.4, 27.1, 27.0, 22.6, 14.1. MALDI-TOF MS: m/z = 1241.5 ([M]+1, $C_{73}H_{71}N_7Pt$ requires 1240.5).

General Procedure of Consecutive Titration. The titrand solutions of **1** and **2** (100 mL) were freshly prepared in CH_2Cl_2 before the consecutive titration experiment. The 0.05 mol·dm^{-3} $HClO_4$ and 0.05 mol·dm^{-3} KOH titrant solutions were also prepared in CH_3OH. Acid−base titration was adopted for **1**, while Zn^{2+}-acid-base and acid-Zn^{2+}-base sequence titrations were designed for **2**. Absorption and emission spectra were recorded simultaneously after each addition (10 μL) of the corresponding titrant solution. Each titration step was stopped after no more changes were observed in the absorption and emission properties. The selectivity of protonated **2** toward different metal cations was monitored by the parallel photoluminescence (PL) experiment under the same instrument condition, in which 0.5 equiv of the metal ions was added in each titrand solution containing 1.5 × 10^{-5} mol·dm^{-3} **2**.

Physical Measurements and Instrumentation. ^1H and ^{13}C NMR spectra were recorded on Bruker AV 300 and 400 spectrometers and referenced with respect to tetramethylsilane, $Si(CH_3)_4$, internal standard. Elemental analyses were performed using a Bio-Rad Co

DOI: 10.1021/acs.inorgchem.5b00756
Inorg. Chem. 2015, 54, 7774−7782

elemental analytical instrument. MALDI-TOF MS analyses were performed on a Bruker Autoflex III mass spectrometer. UV−vis absorption spectra were obtained using a PerkinElmer Lambda 650s ultraviolet−visible (UV−vis) spectrophotometer. PL spectra were performed on a PerkinElmer LS50B spectrometer. Cyclic voltammetry (CV) was conducted on a CHI660A electrochemical workstation in CH_2Cl_2 solution with a three-electrode electrochemical cell using a platinum disk electrode (Φ = 3.0 mm), a saturated calomel electrode (SCE), and a Pt wire as the working electrode, the reference electrode, and the counter electrode, respectively. $^nBu_4NClO_4$ (0.1 mol·dm^{-3}) was used as the supporting electrolyte, and the scan rate was 50 mV·s^{-1}.

RESULTS AND DISCUSSION

Synthesis and Characterization. The syntheses of complexes **1** and **2** explored in this work are shown in Scheme 1. The powerful palladium-catalyzed amination method and the efficient $Pd(OAc)_2$/DPEphos catalyst/ligand system[10] were adopted to facilitate the condensation of *N*′-(*tert*-butoxycarbonyl)-*N*′-(phenyl)-*p*-phenylenediamine with 4-(*p*-bromophenyl)-6-phenyl-2,2′-bipyridine. The *tert*-butyl carbamate (BOC) groups of the resulting intermediate was removed quantitatively by thermolysis[11] under an inert atmosphere at 185 °C for 12 h and then reaction with 1-bromooctane to afford ligand HL. The cyclometalated Pt(II) chloride [(L)PtCl] was synthesized by refluxing HL and K_2PtCl_4 in glacial acetic acid for 12 h. The 4′-{4-[2-(trimethylsilyl)-1-ethynyl]phenyl}-2,2′:6′,2″-terpyridine compound was prepared via the palladium-catalyzed cross-coupling reaction[12] in good yield by treatment of the corresponding bromo-substituted ligand with (trimethylsilyl)acetylene at 75 °C in the presence of catalytic amounts of $Pd(OAc)_2/PPh_3$/CuI and diisopropylamine as base, which can generate the active palladium(0) catalyst in situ. Followed by deprotection of the trimethylsilyl group with K_2CO_3 in CH_3OH/THF (1/1, v/v) solution, 4′-(4-ethynylphenyl)-2,2′:6′,2″-terpyridine was prepared in excellent yield of 91%. Finally reaction of [(L)PtCl] with phenylacetylene and 4′-(4-ethynylphenyl)-2,2′:6′,2″-terpyridine to obtain complexes **1** and **2** by Sonogashira's method, respectively. Both of them have good solubility in CH_2Cl_2 and were characterized by ^{1}H NMR, ^{13}C NMR, and MALDI-TOF MS.

Photophysical Properties of 1 and 2. The UV−vis absorption spectra of complexes **1** and **2** in CH_2Cl_2 solution exhibit intense bands at 250−400 nm and less intense bands at 400−550 nm (Table 1 and Figure S1 in Supporting Information). With reference to previous spectroscopic work on phenylbipyridyl platinum(II) phenylacetylides,[13] the high-energy intense absorption bands are clearly assigned to the singlet $\pi \rightarrow \pi^*$ intraligand (IL) transitions of phenylbipyridine (C^N^N) and alkynyl (C≡C−Ar) ligands. Noticeably, compared with that of complex [(ph-C^N^N)Pt(C≡C−C_6H_5)] (λ_{max} = 456 nm, ε = 7.53 × 10^3 dm^3·mol^{-1}·cm^{-1}),[9b] the low-energy absorption bands of **1** (λ_{max} = 462 nm, ε = 25.8 × 10^3 dm^3·mol^{-1}·cm^{-1}) and **2** (λ_{max} = 470 nm, ε = 31.5 × 10^3 dm^3·mol^{-1}·cm^{-1}) are apparently red-shifted and have 3−4 times increase in intensity after the introduction of arylamine dimer. This observation is consistent with previous work, where introduction of the electron-donating dimethylamino or diphenylamino groups at the para-position of ph-TPY,[14] alkoxyl substituent on 4,6-diphenyl-2,2′-bipyridine ligand,[15] and N-alkyl substituted arylamino or bis(arylamino) units at the 4-position of 6-phenyl-2,2′-bipyridine (C^N^N)[9b] also led to similar effects. Such behavior is strongly indicative of the π(bis(arylamine)) → π^*(C^N^N) intraligand charge transfer (ICT) transition involved in their low-energy bands, overlapping with the well-known spin-allowed singlet dπ(Pt) → π^*(C^N^N) metal-to-ligand charge transfer (MLCT) and π(C≡C−Ar) → π^*(C^N^N) ligand-to-ligand charge transfer (LLCT) transitions. The low-energy absorption bands obey Beer's law in the range from 1 × 10^{-6} to 1 × 10^{-4} mol·dm^{-3}, suggesting no dimerization or oligomerization of the two complexes within this concentration range. Compared to **1**, an unexpected 8 nm red shift of the low-energy absorption band is observed for **2**, which differs from the hypsochromic effect of incorporation of electron-withdrawing groups at the para-position of phenylacetylide ligand in [(C^N^N)Pt(C≡C−C_6H_5)][13] and [(TPY)Pt(C≡C−C_6H_5)]$^+$.[16] This is likely attributed to the further extended π-conjugated system and the resulting intramolecular D(bis(arylamine))−A(TPY) interaction[17] via the planar [(C^N^N)Pt(C≡C−C_6H_5)] moiety after the introduction of TPY unit.

Excited at 450 nm, which is into their MLCT absorption bands, both of them have no emission in fluid solution at room temperature. But strong emissions (λ_{max} = 578 nm for **1** and 580 nm for **2**) are resumed in acidic media, which will be described in detail later.

The electrochemical behaviors of HL, **1**, and **2** were also investigated by CV (Figure 1), and the data are listed in Table 2. The cyclic voltammogram of HL shows a reversible redox wave (ΔE = 55 mV, $i_{p,a}/i_{p,c}$ = 1.1) at $E_{1/2}$ = +0.01 V and an irreversible anodic wave at $E_{p,a}$ = +0.49 V. Because the oxidation potential of the (ph-C^N^N) ligand is beyond the potential window of the solvent, the two redox waves of HL are involved in the consecutive single-electron processes to form the dication radical species.[18] Complex **1** also displays the two

Table 1. UV−vis Absorption and Photoluminescence (PL) Data of the Ligand and Pt (II) Complexes in CH_2Cl_2 Solutions at Room Temperature

compound	$\lambda_{max,\ abs}$ (/nm)(ε × 10^{-3}/dm^3·mol^{-1}·cm^{-1})	$\lambda_{max,em}$ (/nm)
HL	357(27.9), 295(29.5), 247(36.7)	403
[(ph-C^N^N)Pt(C≡C−C_6H_5)]	456 (7.53), 370 (sh, 13.4), 339 (19.0), 286 (52.4)	598
1	462 (25.8), 375 (22.7), 323 (sh, 35.7), 286 (58.3)	no emission
2	470 (31.5), 373 (sh, 29.5), 333 (52.2), 293 (60.6)	no emission

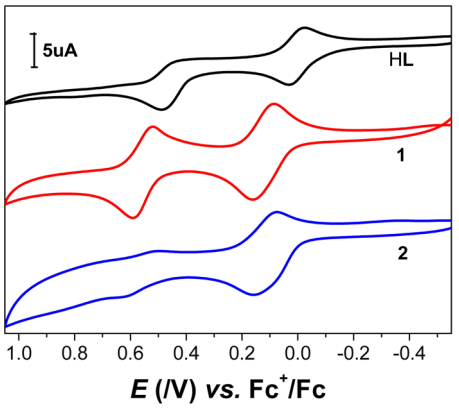

Figure 1. Cyclic voltammograms of HL, **1**, and **2** on Pt electrodes.

DOI: 10.1021/acs.inorgchem.5b00756
Inorg. Chem. 2015, 54, 7774−7782

Table 2. Electrochemical Data[a] of the Ligand and Pt(II) Complexes

compound	oxidation, $E_{p,a}$ (/V)[b] ligand-based	oxidation, $E_{p,a}$ (/V)[b] metal-based	HOMO[c] (eV)	E_g[c] (eV)	LUMO[c] (eV)
HL	+0.03, +0.49		−4.7	3.1	−1.6
[(ph-C^N^N)Pt(C≡C−C_6H_5)]		+0.40	−5.1	2.4	−2.7
1	+0.16, +0.59	overlapped	−4.8	2.4	−2.4
2	+0.16	+0.62	−4.8	2.3	−2.5

[a]Determined in CH_2Cl_2 at room temperature with 0.1 mol·dm^{-3} $^nBu_4NClO_4$ as supporting electrolyte, scanning rate: 50 mV·s^{-1}. [b]Values are listed versus Fc^+/Fc ($E_{1/2}$ = +0.55 V vs saturated calomel electrode (SCE)). [c]The HOMO levels are calculated from the onset values of their first anodic waves according to the equation $E = -(E_{onset} + 4.25)$ eV, while the LUMO levels are calculated from their spectroscopic energy gaps (E_g).

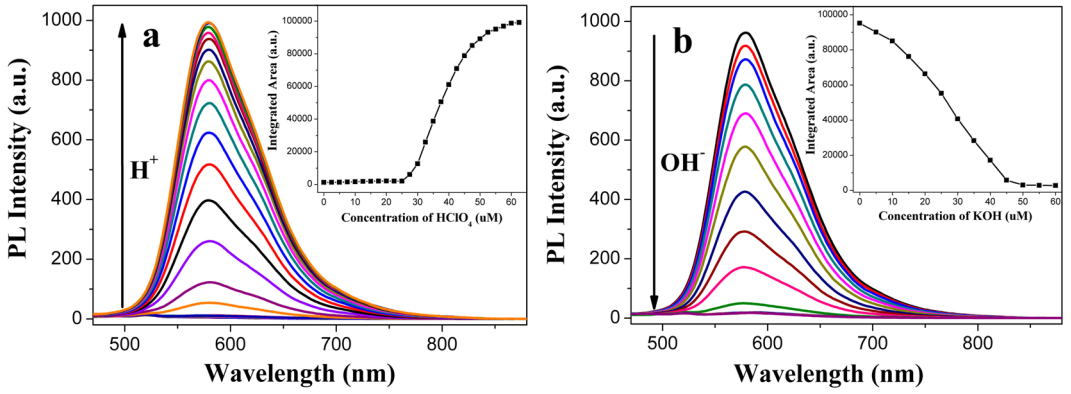

Figure 2. Influence of consecutive H^+ (a) and OH^- (b) titrations on the PL spectra of 1.71 × 10^{-5} mol·dm^{-3} **1** in CH_2Cl_2/CH_3OH solution. The insets show plots of integrated area of the emission wave in range of 500−800 nm vs the concentration of $HClO_4$ and KOH titrants, respectively.

redox waves with clearly positive shifts of their potentials. Because of overlapping with the redox waves of the bis(arylamine) unit, the Pt(II)-based oxidation wave is not observed. With introduction of the electron-withdrawing TPY group at the para-position of phenylacetylide ligand, complex **2** has a united double-electron oxidation wave (the charge ratio of the broad oxidation wave at $E_{p,a}$ = +0.16 V and the reduction wave at $E_{p,c}$ = +0.08 V is 1.8) of the bis(arylamine) unit at $E_{p,a}$ = +0.16 V and a weak Pt(II)-based oxidation wave at $E_{p,a}$ = +0.62 V. The latter one is significantly anodic shifted with reference to that ($E_{p,a}$ = +0.40 V) of complex [(ph-C^N^N)Pt(C≡C−C_6H_5)]. These changes also suggest the strong D−π−A interactions of this three-component system.

Acid−Base Titration of 1. Continuous acid titration was first performed for the reference complex **1** in CH_2Cl_2/CH_3OH solution (Figure 2a). No apparent emission is observed at beginning, but a clear emission wave at λ_{max} = 578 nm is present when $HClO_4$ concentration reaches to ∼2.5 × 10^{-5} mol·dm^{-3}. As further increase of the acid concentration, the emission intensity is gradually increased and finally reaches its maximum at the second turning point of ∼5.0 × 10^{-5} mol·dm^{-3} $HClO_4$ (Figure 2a, inset). The two acid concentrations should correspond to initial and complete protonation of the bis(arylamine) donor, respectively. Simultaneously, gradual intensity decrease and apparent blue shift of its low-energy absorption band are observed during the acid titration procedure (Supporting Information, Figure S2). The absorption and emission properties of completely protonated **1** are close to those of the phenylbipyridyl Pt(II) phenylacetylides with electron-withdrawing groups at 4-position.[13] These results suggest that upon protonation, the MLCT emission from the cyclometalated Pt(II) acetylide unit is recovered. The acid-dependent emission (Figure 2b) and absorption (Supporting Information, Figure S3) changes are found to be fully reversible upon addition of the KOH titrant solution.

Zn^{2+}-Acid-Base Sequence Titration of 2. As shown in Figure 3, the low-energy absorption band (λ_{max} = 470 nm) of **2**

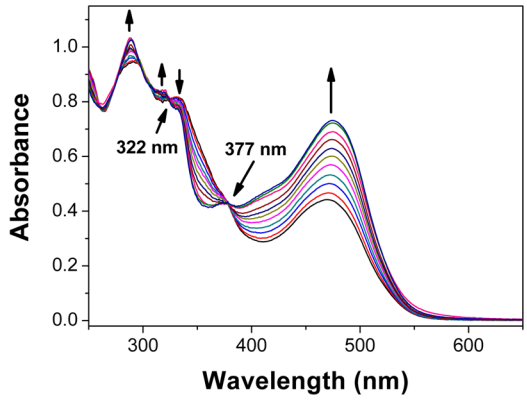

Figure 3. Influence of the $Zn(ClO_4)_2$ titrant on the UV−vis absorption spectra of 1.50 × 10^{-5} mol·dm^{-3} **2** in CH_2Cl_2/CH_3OH solution.

is gradually increased with continuous addition of Zn^{2+} and finally reaches its maximum. A perfect linear relationship (R = 0.99956) is obtained from the absorption titration data for the plot measured ($A - A_0$) at 470 nm as a function of [Zn^{2+}] (from 0 to 6.75 × 10^{-6} mol·dm^{-3}; Supporting Information Figure S4), and the limit of detection (LOD) is 2.15 × 10^{-7} mol·dm^{-3}. The two isosbestic points at 377 and 322 nm suggest the formation of zinc complex. The method of continuous variation (Job's plot; Figure 4) shows the 2:1 stoichiometry of **2** and Zn^{2+} ion, indicating that the added zinc ions bond to the free TPY receptor of **2** to form the

DOI: 10.1021/acs.inorgchem.5b00756
Inorg. Chem. 2015, 54, 7774−7782

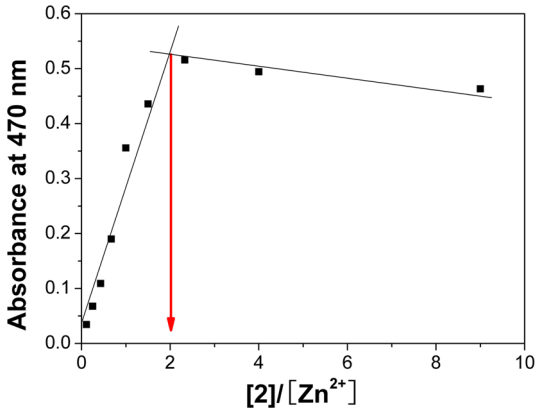

Figure 4. Job's plot of **2** and Zn^{2+} in neutral CH_2Cl_2/CH_3OH solution.

heterotrinuclear complex (Pt−Zn−Pt) containing a $[Zn(TPY)_2]^{2+}$ core. The association constant of **2** with Zn^{2+}, $K_a = 6.86 \times 10^9$ $mol^{-2}\cdot dm^6$, is also determined by linear least-squares fitting of the absorption titration data[19] (Supporting Information, Figure S5). This value is comparable to that ($(4.3 \pm 0.6) \times 10^9$ $mol^{-2}\cdot dm^6$) of triphenylamine (TPA) modified TPY with Zn^{2+} in ethanol.[20] Though the resulting heterotrinuclear complex (Pt−Zn−Pt) has no emission in neutral solution, a strong emission wave at λ_{max} = 576 nm gradually appeared and increased upon protonation of the bis(arylamine) donors in this complex (Figure 5a), which can also be quenched by adding the KOH titrant solution (Figure 5b). Additionally, a perfect linear relationship (R = 0.99981) between PL intensity and $[OH^-]$ (from 1.0×10^{-5} to 6.5×10^{-5} $mol\cdot dm^{-3}$) is obtained from the quenching titration data (Supporting Information, Figure S6), and the LOD is 1.09×10^{-6} $mol\cdot dm^{-3}$. Therefore, the thusly obtained heterotrinuclear complex (Pt−Zn−Pt) shows potential usage as a H^+-triggered turn-off phosphorescent sensor for OH^- ions. Furthermore, the phosphorescence of this system can be switched on and off upon successive additions of H^+ and OH^- ions.

Acid-Zn^{2+}-Base Sequence Titration of 2. The opposite sequence titration experiment was also conducted in CH_2Cl_2/CH_3OH solution containing 1.39×10^{-5} $mol\cdot dm^{-3}$ **2**. Compared with those of reference **1**, similar acid-dependent emission and absorption changes are observed for **2**, besides that (1) higher $HClO_4$ concentration (~5.0×10^{-5} $mol\cdot dm^{-3}$) is needed to initially recover its emission at λ_{max} = 580 nm (Figure 6a), suggesting the presence of a two-step protonation process including the previous bis-protonation of the free TPY moiety[20] and then the bis-protonation of the bis(arylamine) unit. (2) During the first bis-protonation step, the low-energy absorption band of **2** is gradually increased and red-shifted with the addition of $HClO_4$ solution (Figure 7), likely resulting from the enhanced D−A interaction between the unprotonated bis(arylamine) donor and the bis-protonated TPY acceptor.[21] (3) A broad and weak absorption band at long-wavelength region is clearly present after complete protonation of **2** (Figure 7), which is consistent with the appearance of free carriers in the highly conductive state of organic conducting polymers or their hybrids.[22]

Consecutive titration of Zn^{2+} into the completely acidified **2** solution results in further increasing its PL emission with slight blue shift ($\Delta\lambda_{max}$ = 2 nm) of its maximum emission wavelength (Figure 6a) and its low-energy absorption intensity with disappearance of the long-wavelength band (Supporting Information, Figure S7). Terpyridines are well-known to possess quite high affinity for Zn^{2+} and the 2:1 complexes that are usually formed, just like the above-mentioned coordination behavior of **2** with Zn^{2+} in neutral solution. But in this system, an unusual 5−6:1 stoichiometry of protonated **2** and Zn^{2+} ion is proved by the Job's plot (Figure 8) and the continuous titration data (Figure 9), suggesting the protons previously bonded to the free TPY receptor are partially replaced by the added zinc ions to form the heterotrinuclear complexes (Pt−Zn−Pt). The competition effect of concomitant protons and Zn^{2+} ions results in a near S-shape titration curve (Figure 6a, inset), which is different than the linear relationship of **2** and Zn^{2+} in neutral solution mentioned above. It is difficult to use it to accurately calculate the association constant of **2** with Zn^{2+} in acidic solution. But a good linear relationship can be obtained from the emission titration data by plotting the measured $[1/(I - I_0)]$ at 578 nm as a function of $1/[Zn^{2+}]$, using the well-known Benesi−Hildebrand expression (Supporting Information, Figure S8).[23] So the apparent association constant of protonated **2** with Zn^{2+}, $K_a = 3.54 \times 10^5$ $mol^{-1}\cdot dm^3$ (R = 0.99766), is calculated from the slope and intercept of this linear plot, and the LOD is 1.33×10^{-7} $mol\cdot dm^{-3}$ (Supporting Information, Figure S9). Remarkably, the 2.4-fold luminescence intensity enhancement (I/I_0) is finally obtained, though the formation of the heterotrinuclear complex (Pt−Zn−Pt) is seriously inhabited by protons. This is likely

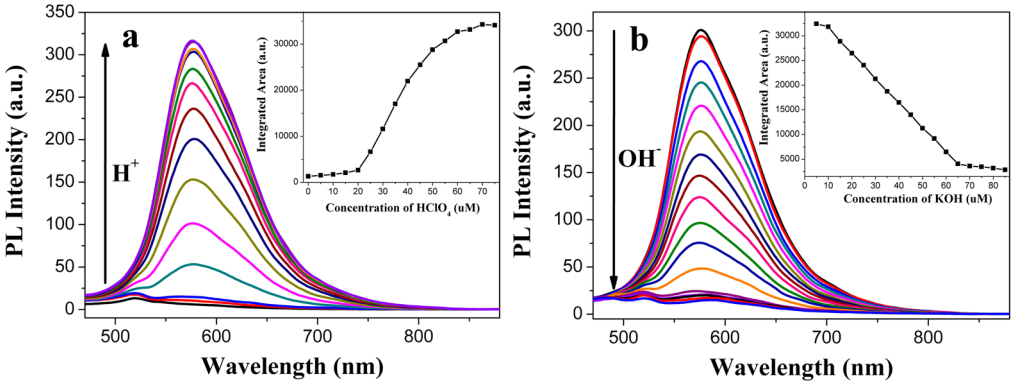

Figure 5. Influence of consecutive H^+ (a) and OH^- (b) titrations on the PL spectra of heterotrinuclear complex (Pt−Zn−Pt) in CH_2Cl_2/CH_3OH solution. (insets) Plots of integrated area of the emission wave in range of 500−800 nm vs the concentration of $HClO_4$ and KOH titrants, respectively.

DOI: 10.1021/acs.inorgchem.5b00756
Inorg. Chem. 2015, 54, 7774−7782

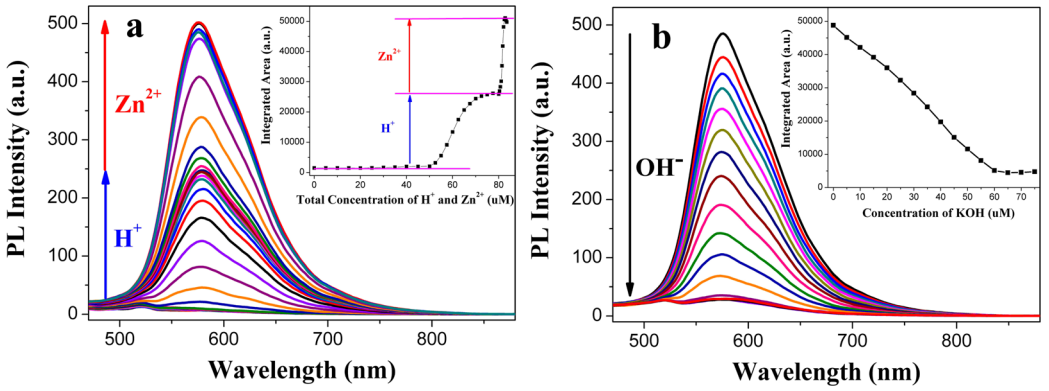

Figure 6. Influence of consecutive H^+, Zn^{2+} (a), and OH^- (b) titrations on the PL spectra of 1.39×10^{-5} mol·dm^{-3} **2** in CH_2Cl_2/CH_3OH solution. (insets) Plots of integrated area of the emission wave in range of 500−800 nm vs the concentration of $HClO_4$, $Zn(ClO_4)_2$, and KOH titrants, respectively.

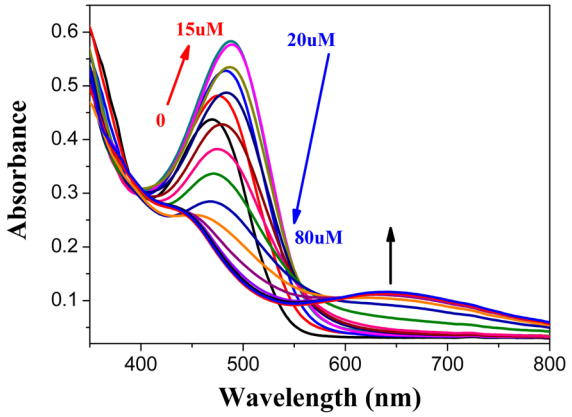

Figure 7. Influence of the concentration of $HClO_4$ titrant on the UV−vis absorption spectra of 1.39×10^{-5} mol·dm^{-3} **2** in CH_2Cl_2/CH_3OH solution.

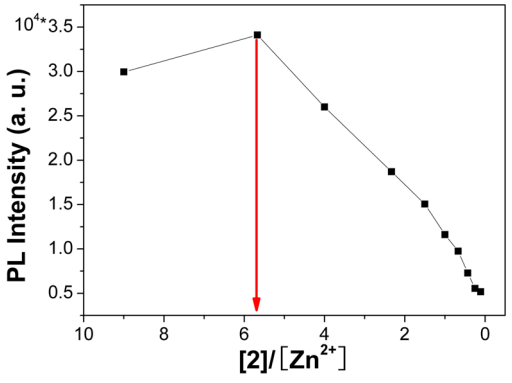

Figure 8. Job's plot of **2** and Zn^{2+} in acidic CH_2Cl_2/CH_3OH solution.

due to the presence of the intramolecular energy transfer (IET) process from the $[Zn(TPY)_2]^{2+}$ core to the completely protonated $[(L)Pt(C{\equiv}C{-}C_6H_5)]$ units at two ends, as well as the higher rigidity of the Pt−Zn−Pt complex.[24] The supposed IET mechanism is partially supported by the overlapping effect between the emission band of $[Zn(ph\text{-}TPY)_2]^{2+}$ complex and the low-energy absorption band of the completely protonated **1** (Supporting Information, Figure S10). The interesting two-step luminescence enhancement property (Figure 6a, inset) of **2** is also found to be fully quenched upon addition of the KOH titrant solution (Figure 6b). Additionally,

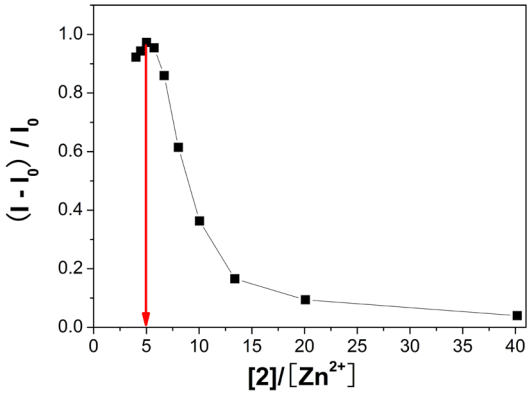

Figure 9. Changes of PL intensity vs the ratio of protonated **2** and Zn^{2+}.

a good linear relationship (R = 0.99835) between PL intensity and $[OH^-]$ (from 0 to 6.0×10^{-5} mol·dm^{-3}) is also obtained from the quenching titration data (Supporting Information, Figure S11), and the LOD is 3.51×10^{-6} mol·dm^{-3}. Therefore, complex **2** performs a H^+-triggered turn-on phosphorescence sensing behavior for Zn^{2+}, and the resulting system can be probably used as a turn-off phosphorescent sensor of OH^- ions.

Proton-Induced Suppression of the Intraligand Charge Transfer Process in 1 and 2. Complexes **1** and **2** have no emission in CH_2Cl_2 solution at room temperature, but strong emissions are resumed in acidic media. To explain the emission properties, the highest occupied molecular orbital (HOMO) and lowest unoccupied molecular orbital (LUMO) levels of **1** and **2** were estimated from their electrochemical and spectroscopic data[25] (Table 2). Previous experiment studies and theoretical calculations on the frontier molecular orbitals of phosphorescence cyclometalated Pt(II) acetylide reveal that the HOMO is basically Pt(II) acetylide-based, and the LUMO predominantly corresponds to the π^* orbitals of cyclometalated ligands.[15,26] When the bis(arylamine) unit is attached to (ph-C^N^N) ligand, each of **1** and **2** shows an elevated HOMO energy level (−4.8 eV) relative to $[(ph\text{-}C\text{^}N\text{^}N)Pt(C{\equiv}C{-}C_6H_5)]$ (−5.1 eV). The strong electron-donating substituent raises the HOMO level to such an extent that the lowest-energy excited state corresponds to the ICT transition, resulting in the quenching of their MLCT emissions. Upon protonation, H^+ attracts the lone pair of the nitrogen atoms of the bis(arylamine) group to reduce their electron-donating

DOI: 10.1021/acs.inorgchem.5b00756
Inorg. Chem. 2015, 54, 7774−7782

Scheme 2. Proposed Mechanism for Zn^{2+} Sensing by Probe 2

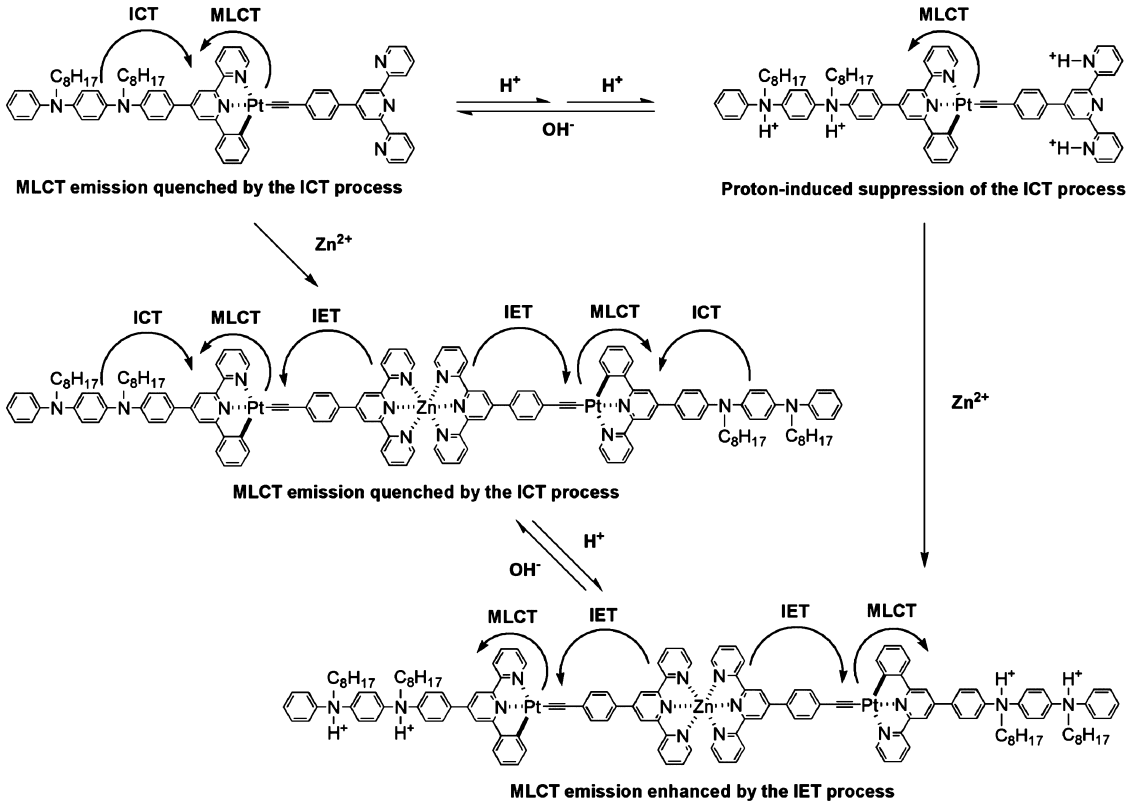

character, so the ICT process can be suppressed, and their MLCT emissions are recovered, as observed above for **1** and **2** as well as the heterotrinuclear Pt−Zn−Pt complex. Although fluorophores with ICT excited states have been previously considered for metal ion sensing,[14,16] the three-component system **2** displays an unusual multichannel phosphorescence switched by the MLCT, ICT, and IET transitions (Scheme 2), which is expected to use as a H^+/OH^--controlled sensor for metal ions.

Selectivity. The binding behaviors of protonated **2** toward different metal cations (0.5 equiv of **2**) were monitored using PL spectroscopy under the same condition. As shown in Figure 10, only Pb^{2+} elicits no significant luminescence quenching or enhancing responses. As expected, other common transition metal ions, such as Mn^{2+}, Fe^{2+}, Co^{2+}, Ni^{2+}, and Cu^{2+}, exhibit dramatic luminescence quenching responses, because these metal ions possess low-energy excited states and can be involved in the photoinduced energy/electron transfer processes between the phosphorescent Pt(II) complex units and the metal-TPY complex core.[27] Surprisingly, alkali (Na^+ and K^+) and alkali-earth (Mg^{2+} and Ca^{2+}) ions also cause its phosphorescence quenching. But the luminescence enhancement effect is observed in the presence of Zn^{2+} or Cd^{2+} ion with the filled d^{10} electronic configuration. Unexpectedly, an improved selectivity of Zn^{2+} over Cd^{2+} by 5.1-fold is obtained, compared with those of TPY and its analogue-based chemosensors.[8,16,20]

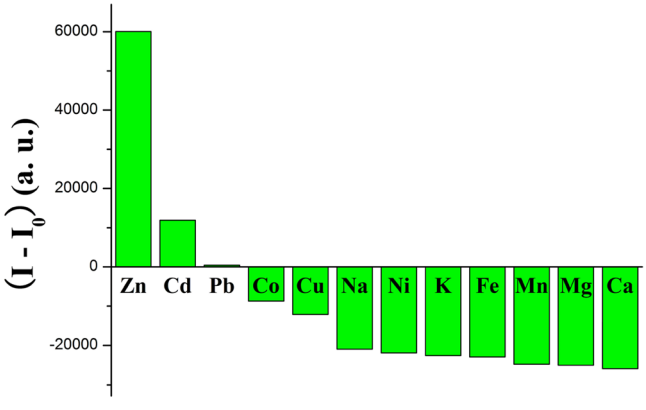

Figure 10. PL response of protonated **2** to various metal ions.

CONCLUSION

In this paper, we have developed a novel cyclometalated Pt(II) acetylide derivative bearing a bis(arylamine) donor and a TPY receptor, which exhibits the H^+-triggered, Zn^{2+}-enhanced, and OH^--quenched phosphorescence properties following an unusual multichannel sensing mode by switching the $d\pi(Pt) \rightarrow \pi^*(C^N^N)$ MLCT, the $\pi(bis(arylamine)) \rightarrow \pi^*(C^N^N)$ ICT, and the $[Zn(TPY)_2]^{2+}$-to-$[(C^N^N)Pt(C{\equiv}C{-}C_6H_5)]$ IET transitions. Furthermore, with introduction of the nonselective TPY receptor into the bis(arylamine) functionalized cyclometalated Pt(II) acetylide, an unexpected Zn^{2+}-selective luminescence chemosensor has been exploited in acidic solution. These results suggest its potential usage as the H^+/OH^--controlled ON/OFF luminescence chemosensor for zinc ion in both biological and environmental applications.

ASSOCIATED CONTENT

Supporting Information

Spectroscopic studies and titration analysis of complexes **1** and **2**. The Supporting Information is available free of charge on the

DOI: 10.1021/acs.inorgchem.5b00756
Inorg. Chem. 2015, 54, 7774−7782

ACS Publications website at DOI: 10.1021/acs.inorgchem.5b00756.

AUTHOR INFORMATION

Corresponding Author

*E-mail: qiudf2008@163.com.

Notes

The authors declare no competing financial interest.

ACKNOWLEDGMENTS

We thank the Natural Science Foundation of Henan Province (102300410221), the Natural Science Foundation of Nanyang Normal University (ZX2010012), and the Young Core Instructor Project of the Education Commission of Henan Province for funding support.

REFERENCES

(1) (a) Frederickson, C. J.; Koh, J. Y.; Bush, A. I. *Nat. Rev. Neurosci.* **2005**, *6*, 449. (b) Hambidge, M. *J. Nutr.* **2000**, *130*, 1344S. (c) Sandström, B. *Food Nutr. Bull.* **2001**, *22*, 133.

(2) (a) Formica, M.; Fusi, V.; Giorgi, L.; Micheloni, M. *Coord. Chem. Rev.* **2012**, *256*, 170. (b) Demas, J. N.; DeGraff, B. A. *Coord. Chem. Rev.* **2001**, *211*, 317. (c) Keefe, M. H.; Benkstein, K. D.; Hupp, J. T. *Coord. Chem. Rev.* **2000**, *205*, 201.

(3) (a) Roy, N.; Pramanik, H. A. R.; Paul, P. C.; Singh, T. S. *Spectrochim. Acta, Part A* **2015**, *140*, 150. (b) Li, P.; Zhou, X.; Huang, R.; Yang, L.; Tang, X.; Dou, W.; Zhao, Q.; Liu, W. *Dalton Trans.* **2014**, *43*, 706. (c) Wu, K.; Gao, Y.; Yu, Z.; Yu, F.; Jiang, J.; Guo, J.; Han, Y. *Anal. Methods* **2014**, *6*, 3560. (d) Gupta, V. K.; Singh, A. K.; Kumawat, L. K. *Sens. Actuators, B* **2014**, *204*, 507. (e) Zhang, M.; Lu, W.; Zhou, J.; Du, G.; Jiang, L.; Ling, J.; Shen, Z. *Tetrahedron* **2014**, *70*, 1011. (f) Sarkar, D.; Pramanik, A. K.; Mondal, T. K. *RSC Adv.* **2014**, *4*, 25341. (g) Baek, K.; Eom, M. S.; Kim, S.; Han, M. S. *Tetrahedron Lett.* **2013**, *54*, 1654. (h) Kim, J. H.; Noh, J. Y.; Hwang, I. H.; Kang, J.; Kim, J.; Kim, C. *Tetrahedron Lett.* **2013**, *54*, 2415. (i) Zhang, G.; Li, H.; Bi, S.; Song, L.; Lu, Y.; Zhang, L.; Yu, J.; Wang, L. *Analyst* **2013**, *138*, 6163. (j) Sivaraman, G.; Anand, T.; Chellappa, D. *Analyst* **2012**, *137*, 5881. (k) Saha, U. C.; Chattopadhyay, B.; Dhara, K.; Mandal, S. K.; Sarkar, S.; Khuda-Bukhsh, A. R.; Mukherjee, M.; Helliwell, M.; Chattopadhyay, P. *Inorg. Chem.* **2011**, *50*, 1213. (l) Zhu, J. F.; Yuan, H.; Chan, W. H.; Lee, A. W. M. *Org. Biomol. Chem.* **2010**, *8*, 3957. (m) Bencini, A.; Berni, E.; Bianchi, A.; Fornasari, P.; Giorgi, C.; Lima, J. C.; Lodeiro, C.; Melo, M. J.; de Melo, J. S.; Parola, A. J.; Pina, F.; Pina, J.; Valtancoli, B. *Dalton Trans.* **2004**, 2180. (n) Gunnlaugsson, T.; Lee, T. C.; Parkesh, R. *Org. Biomol. Chem.* **2003**, *1*, 3265.

(4) (a) Ma, D. L.; He, H. Z.; Zhong, H. J.; Lin, S.; Chan, D. S. H.; Wang, L.; Lee, S. M. Y.; Leung, C. H.; Wong, C. Y. *ACS Appl. Mater. Interfaces* **2014**, *6*, 14008. (b) Woo, H.; Cho, S.; Han, Y.; Chae, W. S.; Ahn, D. R.; You, Y.; Nam, W. *J. Am. Chem. Soc.* **2013**, *135*, 4771. (c) You, Y.; Cho, S.; Nam, W. *Inorg. Chem.* **2014**, *53*, 1804. (d) You, Y.; Lee, S.; Kim, T.; Ohkubo, K.; Chae, W. S.; Fukuzumi, S.; Jhon, G. J.; Nam, W.; Lippard, S. J. *J. Am. Chem. Soc.* **2011**, *133*, 18328. (e) Lee, P. K.; Law, W. H. T.; Liu, H. W.; Lo, K. K. W. *Inorg. Chem.* **2011**, *50*, 8570.

(5) (a) Lanoë, P. H.; Fillaut, J. L.; Guerchais, V.; Le Bozec, H.; Williams, J. A. G. *Eur. J. Inorg. Chem.* **2011**, *2011*, 1255. (b) Lo, H. S.; Yip, S. K.; Wong, K. M. C.; Zhu, N.; Yam, V. W. W. *Organometallics* **2006**, *25*, 3537. (c) Wong, K. M. C.; Tang, W. S.; Lu, X. X.; Zhu, N.; Yam, V. W. W. *Inorg. Chem.* **2005**, *44*, 1492. (d) Yang, Q. Z.; Wu, L. Z.; Zhang, H.; Chen, B.; Wu, Z. X.; Zhang, L. P.; Tung, C. H. *Inorg. Chem.* **2004**, *43*, 5195. (e) Siu, P. K. M.; Lai, S. W.; Lu, W.; Zhu, N.; Che, C. M. *Eur. J. Inorg. Chem.* **2003**, *2003*, 2749. (f) Yam, V. W. W.; Tang, R. P. L.; Wong, K. M. C.; Lu, X. X.; Cheung, K. K.; Zhu, N. *Chem. - Eur. J.* **2002**, *8*, 4066. (g) Yam, V. W. W.; Tang, R. P. L.; Wong, K. M. C.; Ko, C. C.; Cheung, K. K. *Inorg. Chem.* **2001**, *40*, 571.

(6) (a) Chung, S. K.; Tseng, Y. R.; Chen, C. Y.; Sun, S. S. *Inorg. Chem.* **2011**, *50*, 2711. (b) Wong, K. M. C.; Yam, V. W. W. *Coord. Chem. Rev.* **2007**, *251*, 2477. (c) Han, X.; Wu, L.-Z.; Si, G.; Pan, J.; Yang, Q. Z.; Zhang, L. P.; Tung, C. H. *Chem. - Eur. J.* **2007**, *13*, 1231. (d) Yam, V. W. W.; Chan, K. H. Y.; Wong, K. M. C.; Chu, B. W. K. *Angew. Chem., Int. Ed.* **2006**, *45*, 6169. (e) Wong, K. M. C.; Tang, W. S.; Lu, X. X.; Zhu, N.; Yam, V. W. W. *Inorg. Chem.* **2005**, *44*, 1492.

(7) Muro, M. L.; Diring, S.; Wang, X.; Ziessel, R.; Castellano, F. N. *Inorg. Chem.* **2008**, *47*, 6796.

(8) Lanoë, P. H.; Fillaut, J. L.; Guerchais, V.; Le Bozec, H.; Williams, J. A. G. *Eur. J. Inorg. Chem.* **2011**, *2011*, 1255.

(9) (a) Qiu, D.; Wu, J.; Xie, Z.; Cheng, Y.; Wang, L. *J. Organomet. Chem.* **2009**, *694*, 737. (b) Qiu, D.; Zhao, Q.; Liu, K.; Guo, Y.; Feng, Y. *Chin. J. Struct. Chem.* **2010**, *29*, 1513. (c) Qiu, D.; Cheng, Y.; Wang, L. *Dalton Trans.* **2009**, 3247.

(10) (a) Singer, R. A.; Sadighi, J. P.; Buchwald, S. L. *J. Am. Chem. Soc.* **1998**, *120*, 213. (b) Sadighi, J. P.; Singer, R. A.; Buchwald, S. L. *J. Am. Chem. Soc.* **1998**, *120*, 4960.

(11) Rawal, V. H.; Jones, R. J.; Cava, M. P. *J. Org. Chem.* **1987**, *52*, 19.

(12) Grosshenny, V.; Romero, F. M.; Ziessel, R. *J. Org. Chem.* **1997**, *62*, 1491.

(13) Lu, W.; Mi, B. X.; Chan, M. C. W.; Hui, Z.; Che, C. M.; Zhu, N.; Lee, S. T. *J. Am. Chem. Soc.* **2004**, *126*, 4958.

(14) (a) Chung, S. K.; Tseng, Y. R.; Chen, C. Y.; Sun, S. S. *Inorg. Chem.* **2011**, *50*, 2711. (b) Mahato, P.; Saha, S.; Das, A. *J. Phys. Chem. C* **2012**, *116*, 17448.

(15) Shao, P.; Li, Y.; Azenkeng, A.; Hoffmann, M. R.; Sun, W. *Inorg. Chem.* **2009**, *48*, 2407.

(16) Latouche, C.; Lanoë, P. H.; Williams, J. A. G.; Guerchais, V.; Boucekkine, A.; Fillaut, J. L. *New J. Chem.* **2011**, *35*, 2196.

(17) (a) Jarosz, P.; Lotito, K.; Schneider, J.; Kumaresan, D.; Schmehl, R.; Eisenberg, R. *Inorg. Chem.* **2009**, *48*, 2420. (b) Scarpaci, A.; Monnereau, C.; Hergúe, N.; Blart, E.; Legoupy, S.; Odobel, F.; Gorfo, A.; Pérez-Moreno, J.; Clays, K.; Asselberghs, I. *Dalton Trans.* **2009**, 4538.

(18) Goodson, F. E.; Hauck, S. I.; Hartwig, J. F. *J. Am. Chem. Soc.* **1999**, *121*, 7527.

(19) Valeur, B.; Pouget, J.; Bourson, J.; Kaschke, M.; Ernsting, N. P. *J. Phys. Chem.* **1992**, *96*, 6545.

(20) Goodall, W.; Williams, J. A. G. *Chem. Commun.* **2001**, 2514.

(21) (a) Li, C.; Liu, M.; Pschirer, N. G.; Baumgarten, M.; Müllen, K. *Chem. Rev.* **2010**, *110*, 6817. (b) Qian, G.; Wang, Z. Y. *Chem. - Asian J.* **2010**, *5*, 1006. (c) Bundgaard, E.; Krebs, F. C. *Sol. Energy Mater. Sol. Cells* **2007**, *91*, 954. (d) Fabian, J.; Nakazumi, H.; Matsuoka, M. *Chem. Rev.* **1992**, *92*, 1197.

(22) Kingsborough, R. P.; Swager, T. M. *J. Am. Chem. Soc.* **1999**, *121*, 8825.

(23) (a) Anbu, S.; Ravishankaran, R.; Guedes da Silva, M. F. C.; Karande, A. A.; Pombeiro, A. J. L. *Inorg. Chem.* **2014**, *53*, 6655. (b) Yang, X. B.; Yang, B. X.; Ge, J. F.; Xu, Y. J.; Xu, Q. F.; Liang, J.; Lu, J. M. *Org. Lett.* **2011**, *13*, 2710. (c) Zhu, M.; Yuan, M.; Liu, X.; Xu, J.; Lv, J.; Huang, C.; Liu, H.; Li, Y.; Wang, S.; Zhu, D. *Org. Lett.* **2008**, *10*, 1481.

(24) (a) Bellows, D.; Aly, S. M.; Gros, C. P.; El Ojaimi, M.; Barbe, J. M.; Guilard, R.; Harvey, P. D. *Inorg. Chem.* **2009**, *48*, 7613. (b) Flamigni, L.; Collin, J. P.; Sauvage, J. P. *Acc. Chem. Res.* **2008**, *41*, 857. (c) Li, X. L.; Shi, L. X.; Zhang, L. Y.; Wen, H. M.; Chen, Z. N. *Inorg. Chem.* **2007**, *46*, 10892. (d) Li, X. L.; Dai, F. R.; Zhang, L. Y.; Zhu, Y. M.; Peng, Q.; Chen, Z. N. *Organometallics* **2007**, *26*, 4483. (e) Odobel, F.; Zabri, H. *Inorg. Chem.* **2005**, *44*, 5600.

(25) Zhou, G.; Pschirer, N.; Schöneboom, J. C.; Eickemeyer, F.; Baumgarten, M.; Müllen, K. *Chem. Mater.* **2008**, *20*, 1808.

(26) (a) Latouche, C.; Lanoë, P. H.; Williams, J. A. G.; Guerchais, V.; Boucekkine, A.; Fillaut, J. L. *New J. Chem.* **2011**, *35*, 2196. (b) Wang, X.; Goeb, S.; Ji, Z.; Castellano, F. N. *J. Phys. Chem. B* **2010**, *114*, 14440. (c) Zhou, G. J.; Wang, X. Z.; Wong, W. Y.; Yu, X. M.; Kwok, H. S.; Lin, Z. *J. Organomet. Chem.* **2007**, *692*, 3461.

(27) Fermi, A.; Bergamini, G.; Roy, M.; Gingras, M.; Ceroni, P. *J. Am. Chem. Soc.* **2014**, *136*, 6395.

DOI: 10.1021/acs.inorgchem.5b00756
Inorg. Chem. 2015, 54, 7774−7782